JOURNAL OF GUIDANCE, CONTROL, AND DYNAMICS
Vol. 27, No. 3, May–June 2004

State-Space Approach to Computing Spacecraft Pointing Jitter

David S. Bayard*
Jet Propulsion Laboratory, California Institute of Technology, Pasadena, California 91109

Pointing jitter refers to unwanted line-of-sight motion incurred by a pointing system over a time window of specified duration. Jitter acts to smear images and degrade the quality of science obtainable from camera-type instruments. A recent mathematical expression for finite window pointing jitter involves the frequency-domain integral of a rational polynomial multiplied by a transcendental weighting function. Because of its complexity, the expression is generally evaluated using numerical integration. The main contribution of this paper is a state-space method for evaluating the frequency-domain integral. In particular, an exact state-space expression is developed that can be evaluated by computing a matrix exponential and solving a Lyapunov equation.

I. Introduction

THE issue of pointing jitter is important for essentially all space missions that carry scientific payloads. Consequently, methods to define and evaluate pointing jitter have been addressed in various contexts in the literature.[1–8]

The present paper is concerned with statistical analysis of line-of-sight pointing jitter for imaging-type instruments. In such applications, the jitter acts only over a finite window of time corresponding to the exposure duration. An important finite window definition of rms pointing jitter has been put forth by Sirlin and San Martin[3] (see also Appendix A of Ref. 4) and is becoming adopted by a growing number of Earth-orbiting and deep-space missions. This rms jitter metric captures the dependence of image smear on the duration of a finite time exposure and correctly captures the intuitive notion that jitter in images can be reduced by taking shorter exposures. (In interesting contrast, Ref. 6 shows that certain performance measures for spectroscopic observations improve as the exposures become longer.)

Evaluation of finite window rms pointing jitter is based on a frequency-domain integral involving a rational polynomial multiplied by a transcendental weighting function.[3,4] While extremely useful, this integral representation has complicated its use in practice, typically requiring evaluation by numerical methods.[9] As an alternative to numerical integration, one can make rational approximations to the transcendental weighting function. This approach was suggested in the original papers of Sirlin and San Martin[3] and Lucke et al.[4] and has been discussed and expanded on recently by Pittelkau.[8] The resulting expressions, although approximate, involve a completely rational spectrum and can be integrated directly by algebraic methods (e.g., via a Lyapunov equation).

While numerical integration and rational approximation methods can be made to work in practice, it leaves open the question of whether an exact method can be found for evaluating the jitter integral that does not require numerical integration. The present paper will introduce such an exact expression based on a state-space approach. The state-space framework is useful because it allows one to draw from a wealth of results already developed for covariance analysis and discretization of continuous-time systems (cf. Ref. 10). The state-space expression is applicable to stationary processes with arbitrary rational spectrum, which includes a wide range of pointing processes occurring in practice. The main result was first proved in an engineering report,[11] and appeared subsequently in a conference paper.[7]

Background on pointing jitter is given in Sec. II. The main result for computing pointing jitter is given in Sec. III. Examples are given in Sec. IV that compare the methods in first-order and second-order state-space models. Conclusions are postponed until Sec. V, and Appendix A provides a detailed proof of the main result.

II. Background

A. Pointing Process

Physically, a pointing process is defined by the motion that a camera or instrument boresight undergoes as a function of time. It will be assumed that the pointing process defined earlier can be suitably approximated by a wide-sense stationary random process (cf. Ref. 12). This permits all of the pointing control definitions to be made in precise mathematical terms.

The wide-sense stationarity assumption is relatively mild in that it requires only that the process is stationary in its first and second moments (as opposed to strict-sense stationarity, which requires stationarity in all moments) and does not impose any specific form on the shape of the underlying probability distributions.

B. Pointing Definitions

The per-axis pointing jitter definitions of interest are depicted graphically in Fig. 1. This diagram will be discussed in detail in this section.

Let $n(t)$ be a zero-mean second-order stationary random process such that

$$E[n(t)] = 0 \tag{1}$$

$$R_n(\ell) \triangleq E[n(t)n(t+\ell)] \tag{2}$$

$$S_n(\omega) \triangleq F\{R_n(\ell)\} \tag{3}$$

$$\sigma_n^2 \triangleq R_n(0) < \infty \tag{4}$$

Here the Fourier transform of a signal $x(t)$ is denoted as $X(\omega) = F\{x(t)\}$ and is defined as

$$X(\omega) = F\{x(t)\} = \int_{-\infty}^{\infty} x(t)e^{-j\omega t}\,dt \tag{5}$$

Let b be a constant. Then the pointing process $y(t)$ is defined as

$$y(t) = n(t) + b \tag{6}$$

where the quantity b defines the process mean and the quantity σ_n^2 in Eq. (4), which is the variance of $n(t)$, defines the process variance.

Received 31 May 2003; presented as Paper 2003-5782 at the AIAA Guidance, Navigation, and Control Conference, Austin, TX, 11–14 August 2003; revision received 14 October 2003; accepted for publication 1 November 2003.

*Senior Research Scientist, Autonomy and Control Section, MS 198-326, 4800 Oak Grove Drive; david.bayard@jpl.nasa.gov. Senior Member AIAA.

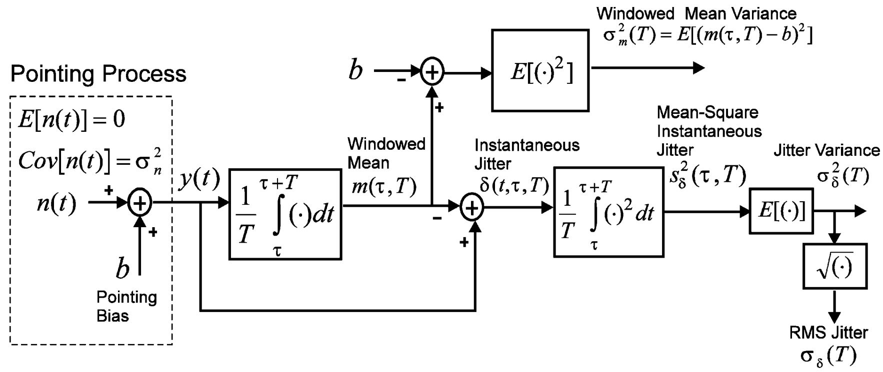

Fig. 1 Pointing jitter definition diagram.

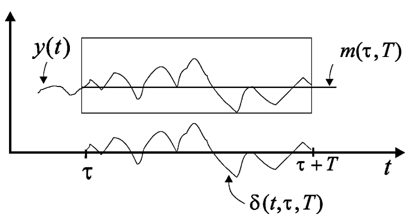

Fig. 2 Definition of instantaneous jitter $\delta(t,\tau,T)$.

Note that a pointing process is ideally zero mean, so that a nonzero b indicates the presence of a pointing bias.

Definition 2.1: The windowed mean over a window of duration T, starting at time τ, is defined as

$$m(\tau,T) = \frac{1}{T}\int_\tau^{\tau+T} y(t)\,\mathrm{d}t \tag{7}$$

□

The windowed mean $m(\tau,T)$ depends on the starting time τ and the duration of the window, T. Because it is a functional of the particular realization of the random process, it is itself a random variable. As such, its variance is defined next based on an ensemble average.

Definition 2.2: The windowed mean variance for windows of size T is defined as

$$\sigma_m^2(T) = E[(m(\tau,T)-b)^2] \tag{8}$$

□

Here, the notational dependence of σ_m^2 on τ has been dropped because the ensemble average in Eq. (8) is taken with respect to y, which is a stationary process.

When an image is taken over an exposure of duration T, it is of interest to know how much smearing occurred due to the instrument boresight "jittering around" during the exposure. This jitter effect is captured by the following definition.

Definition 2.3: The instantaneous jitter over a window starting at time τ and ending at time $\tau+T$ is defined as

$$\delta(t,\tau,T) = y(t) - m(\tau,T) \tag{9}$$

□

The definition of instantaneous jitter is shown pictorially in Fig. 2. It is important to note that the jitter is defined as the instantaneous deviation from the windowed mean $m(\tau,T)$ rather than deviation from the process mean b. This distinction is critical to correctly capture the effect of camera motion on image smearing. Intuitively, an image taken on a finite time interval $t = [\tau, \tau+T]$ collects photons according to $y(t)$ only on this interval and will be centered at the windowed mean rather than the process mean. Accordingly, deviations from the windowed mean cause smear rather than deviations from the process mean.

As shown in Fig. 2, the three time variables t, τ, and T are essential to properly describe δ. Specifically, t is the plotting variable; the window starts at $t=\tau$ and ends at $t=\tau+T$.

The overall effect of the instantaneous jitter on image smearing is captured by its mean-square value in time.

Definition 2.4: The mean-square instantaneous jitter is defined as

$$s_\delta^2(\tau,T) \triangleq \frac{1}{T}\int_\tau^{\tau+T} \delta^2(t,\tau,T)\,\mathrm{d}t \tag{10}$$

□

The mean-square instantaneous jitter $s_\delta^2(\tau,T)$ depends on the starting time τ and the window duration T. Because it is defined in Eq. (10) by a time average taken over a finite time window, it is a random variable that depends on the realization. A more useful statistic is defined next by taking an ensemble average of $s_\delta^2(\tau,T)$ to make it realization independent.

Definition 2.5: The jitter variance is defined as

$$\sigma_\delta^2(T) \triangleq E\left[s_\delta^2(\tau,T)\right] = E\left[\frac{1}{T}\int_\tau^{\tau+T} \delta^2(t,\tau,T)\,\mathrm{d}t\right] \tag{11}$$

□

Here the notational dependence of σ_δ^2 on τ has been dropped because the ensemble average in Eq. (11) is taken with respect to y, which is a stationary process. It is emphasized that, unlike $s_\delta^2(\tau,T)$, the quantity $\sigma_\delta^2(T)$ is not a random quantity. Rather it has been averaged over the ensemble of possible realizations and is a deterministic function of T.

The jitter variance definition in Eq. (11) and its frequency-domain characterization was introduced by Sirlin and San Martin[3] (see also Appendix A of Ref. 4). Their results will be summarized in Sec. II.C.

It is convenient to define the rms jitter which results from simply taking the square root of the jitter variance, that is, Eq. (11).

Definition 2.6: The RMS jitter in a window of duration T is defined as,

$$\sigma_\delta(T) = \sqrt{E\left[\frac{1}{T}\int_\tau^{\tau+T} \delta^2(t,\tau,T)\,\mathrm{d}t\right]} \tag{12}$$

□

The rms jitter is important because it characterizes pointing performance as it affects most cameras and imaging-type instruments. As such, it has been adopted in many recent Jet Propulsion Laboratory (JPL)/NASA space missions for defining pointing requirements [cf. the Cassini mission to Saturn,[13] the Space Infra-Red Telescope Facility (SIRTF),[14,15] and the Space Interferometry Mission[9]; see also Ref. 16].

As one example, the SIRTF mission (i.e., the next and last space telescope in NASA's Great Observatory series) states its pointing requirements as $\sigma_\delta(T = 200\text{ s}) = 0.3$ arcsec and $\sigma_\delta(T = 500\text{ s}) = 0.6$ arcsec, radial.[15] Assuming the two pointing axes have equal variances, this is equivalent to $\sigma_\delta(T = 200\text{ s}) = 0.3/\sqrt{2}$ arcsec and $\sigma_\delta(T = 500\text{ s}) = 0.6/\sqrt{2}$ arcsec, stated as a per-axis pointing requirement. Here the interpretation of $\sigma_\delta(T)$ is exactly as defined in Eq. (12).

Remark 2.1 (Optical Performance): The impact of jitter on optical performance is an important but complex area of study. Some

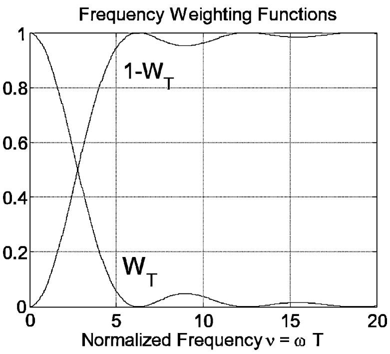

Fig. 3 Frequency weighting $W_T(\omega)$ and $1 - W_T(\omega)$ as a function of $\nu = \omega T$.

discussion can be found in Refs. 4 and 8. In the simplest model (cf. Ref. 4, Appendix B), the jitter motion convolves with the optical point-spread function acting to degrade resolution by increasing the effective point-spread function width. This provides a simple rule of thumb for optical performance degradation as a function of jitter level. However, more accurate optical performance models, particularly in photon-poor situations, may require analyzing photon collection statistics and detailed instrument-specific properties. □

C. Frequency Domain Integrals

Several important frequency-domain integrals have been developed by Sirlin and San Martin[3] (cf. also Appendix A of Ref. 4) for the various jitter expressions defined earlier. These are summarized as follows:

$$\sigma_n^2 = \frac{1}{2\pi}\int_{-\infty}^{\infty} S_n(\omega)\,\mathrm{d}\omega \tag{13}$$

$$\sigma_m^2(T) = \frac{1}{2\pi}\int_{-\infty}^{\infty} S_n(\omega) W_T(\omega)\,\mathrm{d}\omega \tag{14}$$

$$\sigma_\delta^2(T) = \frac{1}{2\pi}\int_{-\infty}^{\infty} S_n(\omega)[1 - W_T(\omega)]\,\mathrm{d}\omega \tag{15}$$

where the weighting function is given by

$$W_T(\omega) = \left[\frac{\sin(\omega T/2)}{\omega T/2}\right]^2 \tag{16}$$

The weighting function $W_T(\omega)$ is plotted in Fig. 3 (vs $\nu = \omega T$ for generic use) and acts as a low-pass filter in the windowed mean variance integral (14).

Its complement, $1 - W_T(\omega)$, is also plotted in Fig. 3 and acts like a high-pass filter in the jitter variance integral (15). This agrees with one's intuitive notion that the jitter that affects image smear is high-frequency in nature. Since $\lim W_T(\omega) \to 1$ as $\lim T \to 0$, one can infer the benefit of using short exposures from Eq. (15), that is,

$$\lim_{T\to 0} \sigma_\delta^2(T) = 0 \tag{17}$$

This confirms one's intuition that the jitter lessens as the exposure becomes shorter.

D. Sinusoidal Disturbances

Sinusoidal disturbances are relatively common on spacecraft. They are induced, for example, by the imbalances of the spinning reaction wheel actuators. The sinusoidal disturbance case has been treated in detail in the original paper by Lucke et al.[9] Their results will be briefly reviewed here to provide a simple example of how to use frequency integral (15).

Consider the case where the pointing process is made up of N sinusoidal disturbances,

$$y = \sum_{i=1}^{N} A_i \cos(\omega_i t + \theta_i) \tag{18}$$

The power spectrum of the sinusoidal sum is given by (cf. Ref. 17)

$$S_n(\omega) = \pi \sum_{i=1}^{N} \frac{A_i^2}{2}[\gamma(\omega - \omega_i) + \gamma(\omega + \omega_i)] \tag{19}$$

where $\gamma(\omega - \omega_i)$ denotes a delta function located at $\omega = \omega_i$ with unity weight. Substituting Eq. (19) into Eq. (15) and using the sifting property of the delta function gives the jitter variance as

$$\sigma_\delta^2(T) = \sum_{i=1}^{N} \frac{A_i^2}{2}[1 - W_T(\omega_i)] \tag{20}$$

This expression is readily evaluated.

E. Two-Dimensional Processes

Jitter motion most generally forms a two-dimensional process (e.g., both up–down, and left–right). The preceeding analysis has only considered the one-dimensional case. However, two-dimensional rms radial jitter motion can be characterized by combining the per-axis rms motions as follows.

Define the radial instantaneous jitter δ_r as

$$\delta_r = \sqrt{\delta_x^2 + \delta_y^2} \tag{21}$$

where δ_x and δ_y are the one-dimensional instantaneous jitters along the x and y (orthogonal) axes, respectively. Intuitively, in a specified finite window of data, the quantity δ_r is the planar distance of the pointing process from the two-dimensional windowed mean.

Define the mean-square instantaneous radial jitter $s_{\delta_r}^2(\tau, T)$ as the mean-square value of δ_r; that is,

$$s_{\delta_r}^2(\tau, T) \triangleq \frac{1}{T}\int_\tau^{\tau+T} \delta_r^2\,\mathrm{d}t = \frac{1}{T}\int_\tau^{\tau+T} \delta_x^2\,\mathrm{d}t + \frac{1}{T}\int_\tau^{\tau+T} \delta_y^2\,\mathrm{d}t \tag{22}$$

Taking the expection of both sides of Eq. (22) gives the radial jitter variance $\sigma_{\delta_r}^2(T)$ as

$$\sigma_{\delta_r}^2(T) \triangleq E\left[s_{\delta_r}^2(\tau, T)\right] = \sigma_{\delta_x}^2(T) + \sigma_{\delta_y}^2(T) \tag{23}$$

or, equivalently,

$$\sigma_{\delta_r}(T) = \sqrt{\sigma_{\delta_x}^2(T) + \sigma_{\delta_y}^2(T)} \tag{24}$$

It is seen that the two-dimensional jitter $\sigma_{\delta_r}(T)$ can be calculated as the rss combination of the per-axis jitters.

Equation (24) can be interpreted as a "radial rms" value for jitter. Its derivation does not require that the two pointing axes are statistically independent or have the same variance or that the underlying probability distributions are known.

Remark 2.2 (Probabilistic Interpretations): Generally speaking, rms metrics are useful because they involve only second-order statistics and do not require any assumptions concerning how the pointing errors are actually distributed. This is an important motivation for studying rms metrics. Of course, much more could be said if the underlying probability distributions happen to be known. For example, if the pointing errors are two-dimensional Gaussian with equal variances, then over a time of T s, a circle of radius $\sigma_{\delta_r}(T)$ centered at the windowed mean will contain the two-dimensional pointing process with 64% probability. Similarly, circles of radius $1.07\sigma_{\delta_r}(T)$, $1.73\sigma_{\delta_r}(T)$, and $2.15\sigma_{\delta_r}(T)$ will contain the pointing process with probabilities of 68.3, 95, and 99%, respectively. Despite these nice interpretations, seasoned practitioners (cf. Ref. 4 p. 567) warn against the ambiguities of making probabilistic interpretations and recommend specifying pointing requirements as rms values for the two axes separately. □

F. Conservation of Variance

By inspection, it is seen that frequency integral (13) can be written as the sum of integrals (14) and (15). This gives the following conservation-of-variance formula:

$$\sigma_n^2 = \sigma_m^2(T) + \sigma_\delta^2(T) \tag{25}$$

This simple relation is important because it says that the process variance σ_n^2 is a conserved quantity. Specifically, in any window of duration T, the pointing process variance σ_n^2 divides itself between the windowed mean variance $\sigma_m^2(T)$ and the jitter variance $\sigma_\delta^2(T)$. Furthermore, this division is generally unequal and such that most of the process variability goes into the windowed mean for short time exposures and into the jitter variance for long exposures; that is,

$$\sigma_n^2 = \lim_{T\to 0} \sigma_m^2(T) = \lim_{T\to\infty} \sigma_\delta^2(T) \tag{26}$$

Because of relation (26), the process variance σ_n^2 is sometimes referred to as the long-term jitter or steady-state jitter.

III. Main Result

A. State-Space Method

The main result is presented, which introduces a state-space method for evaluating integral (14) for the windowed mean variance $\sigma_m^2(T)$, and integral (15) for the windowed jitter variance $\sigma_\delta^2(T)$, without requiring numerical integration. For this presentation, the pointing bias in Eq. (6) is assumed to be zero (i.e., $b = 0$) without loss of generality.

Theorem 3.1: Let the stationary process $y(t)$ be generated by the following state-space model:

$$\dot{x} = Ax + w \tag{27}$$

$$y = Cx \tag{28}$$

Here $A \in \mathcal{R}^{n\times n}$ is an asymptotically stable matrix (i.e., all eigenvalues have strictly negative real parts), $C \in \mathcal{R}^{1\times n}$ is the output matrix, and $w \in \mathcal{R}^{n\times 1}$ is a continuous-time delta-correlated noise process having statistics

$$E[w(t)] = 0 \tag{29}$$

$$E[w(t)w(t+\tau)^T] = Q \cdot \delta(\tau) \tag{30}$$

Here the covariance $Q \in \mathcal{R}^{n\times n}$ can be either a positive definite or positive semidefinite symmetric matrix.

Then assuming system (27)–(28) has reached steady state, the windowed mean variance $\sigma_m^2(T)$ and the windowed jitter variance $\sigma_\delta^2(T)$ of $y(t)$ on the interval $t \in [\tau, \tau + T]$ can be calculated as

$$\sigma_m^2(T) = (2/T^2) C \mathcal{H}_T P_\infty C^T \tag{31}$$

$$\sigma_\delta^2(T) = \sigma_n^2 - \sigma_m^2(T) \tag{32}$$

where

$$\sigma_n^2 = C P_\infty C^T \tag{33}$$

$$\mathcal{H}_T = \int_0^T \int_0^s e^{Ar}\,\mathrm{d}r\,\mathrm{d}s \tag{34}$$

and P_∞ is found by solving the Lyapunov equation

$$0 = AP_\infty + P_\infty A^T + Q \tag{35}$$

Furthermore, the quantity $\mathcal{H}_T$ can be evaluated using any of the following expressions without requiring numerical integration.

Method 1—Matrix Exponential:

$$\mathcal{H}_T = A^{-2}(e^{AT} - I - AT) \tag{36}$$

Method 2—Inverse Laplace Transform:

$$\mathcal{H}_T = \mathcal{L}^{-1}\{(1/s^2)(sI - AT)^{-1}\} \tag{37}$$

Method 3—Augmented Matrix Exponential: $\mathcal{H}_T$ is the upper right $n \times n$ submatrix of the matrix exponential

$$e^{XT} = \begin{bmatrix} F_1 & G_1 & \mathcal{H}_T \\ 0 & F_2 & G_1 \\ 0 & 0 & F_3 \end{bmatrix} \tag{38}$$

where $X \in \mathcal{R}^{3n\times 3n}$ is defined as (denoting $\mathcal{I}$ as the $n \times n$ identity matrix, and $\mathcal{O}$ as an $n \times n$ zero matrix),

$$X = \begin{bmatrix} \mathcal{O} & \mathcal{I} & \mathcal{O} \\ \mathcal{O} & \mathcal{O} & \mathcal{I} \\ \mathcal{O} & \mathcal{O} & A \end{bmatrix} \tag{39}$$

□

Proof: See Appendix A.

A particularly useful expression for the jitter variance is given in the following corollary to Theorem 3.1.

Corollary 3.1: If method 1 of Theorem 3.1 is used to compute the quantity $\mathcal{H}_T$, the jitter variance expression becomes

$$\sigma_\delta^2(T) = C[I - (2/T^2)A^{-2}(e^{AT} - I - AT)]P_\infty C^T \tag{40}$$

Proof: Substituting Eqs. (31) and (33) into Eq. (32) from Theorem 3.1 gives

$$\sigma_\delta^2(T) = C[I - (2/T^2)\mathcal{H}_T]P_\infty C^T \tag{41}$$

Substituting the method 1 expression $\mathcal{H}_T = A^{-2}(e^{AT} - I - AT)$ into Eq. (41) gives the desired expression (40). □

Jitter variance expression (40) of Corollary 3.1 is very useful because it shows all of the relevant state-space quantities in a single expression. Moreover, all of the matrix operations required to calculate Eq. (40) are well understood and computable with numerically sound algorithms. Specifically, this involves the computation of the matrix exponential e^{AT} term (cf. Ref. 18), the computation of the steady-state covariance P_∞ via Lyapunov equation (35) (cf. Ref. 19), and the computation of a matrix square inverse A^{-2}. Here it is recommended to invert A first and then square it [i.e., $A^{-2} = (A^{-1})^2$] to avoid squaring the condition number before inversion. It is noted that matrix A is always invertible because it is an asymptotically stable matrix, which by necessity has no zero eigenvalues.

B. Discussion

The main usefulness of the state-space formulation in Theorem 3.1 is that it replaces the weighted frequency integrals (14) and (15) in the expression for jitter variance, with the unweighted time integral of a matrix exponential (i.e., $\mathcal{H}_T$ in Eq. (34)]. Aside from eliminating the transcendental weighting function W_T in Eq. (16) from the problem, the state-space formulation allows one to take advantage of special results available for integrating expressions involving the matrix exponential. Specifically, Theorem 3.1 provides three methods for evaluating $\mathcal{H}_T$ without numerical integration.

Remark 3.1 (Short-Term Jitter): Substituting the expression

$$e^{AT} = I + AT + A^2T^2/2! + A^3T^3/3! + A^4T^4/4! + \cdots \tag{42}$$

into Eq. (40) and rearranging gives

$$\sigma_\delta^2(T) = -(T/3)CAP_\infty C^T - (T^2/12)CA^2P_\infty C^T + \cdots \tag{43}$$

$$= (T/6)CQC^T - (T^2/12)CA^2P_\infty C^T + \cdots \tag{44}$$

where the last relation follows from the symmetric form $C(\cdot)C^T$ of the first term in Eq. (43) and the identity $AP_\infty + P_\infty A^T = -Q$, obtained from Eq. (35). It is seen from Eq. (44) that for small T the jitter variance decreases linearly with the exposure time T. Equivalently, the rms jitter $\sigma_\delta(T)$ decreases as $\sqrt{T}$. □

Remark 3.2 (Long-Term Jitter): For sufficiently large values of T, the quantity e^{AT} becomes negligible, and jitter variance expression (40) reduces to

$$\sigma_\delta^2(T) \simeq CP_\infty C^T + (2/T)CA^{-1}P_\infty C^T + (2/T^2)CA^{-2}P_\infty C^T \tag{45}$$

$$\simeq CP_\infty C^T - (1/T)CA^{-1}QA^{-T}C^T + (2/T^2)CA^{-2}P_\infty C^T \tag{46}$$

where the last relation follows from the symmetric form $C(\cdot)C^T$ of the second term in Eq. (45) and the identity $P_\infty A^{-T} + A^{-1}P_\infty = -A^{-1}QA^{-T}$, obtained from Eq. (35). It is seen from Eq. (46) that for large T the jitter variance decreases from the full process variance $CP_\infty C^T$ by an amount that is reciprocal to T. □

Remark 3.3 (Requirement Scaling): For short exposures, Eq. (44) provides a simple rule for scaling pointing requirements. Specifically, it says that the rms pointing jitter $\sigma_\delta(T)$ for a given pointing process will grow with the square root of the window time T. As an example, if a pointing system meets a "$\sigma_\delta = 0.3$ arcsec over 200 s" jitter requirement, then the same pointing system should meet a $\sigma_\delta = 0.3 \cdot \sqrt{(500/200)} = 0.47$ arcsec requirement over 500 s. It is emphasized that this simple scaling rule only holds if the exposure time T is small compared to the time constants of the pointing process (i.e., as determined by the eigenvalues of A). Otherwise the full expression of Eq. (40) must be invoked to make such a comparison. □

Remark 3.4: A Gaussian assumption has not been required on the noise w in Eqs. (27) and (28). Accordingly, the results of Theorem 3.1 hold for delta-correlated noise with arbitrary probability distributions. □

Remark 3.5 (Symbolic Expressions): For some state-space systems of the form of Eqs. (27) and (28), matrix exponential expression (36) or inverse Laplace transform expression (37) can be computed in symbolic form. This leads to symbolic expressions for the pointing jitter, which may be useful in practice. Two examples of this will be given in Sec. IV. □

Remark 3.6 (Multiple Exposure Times): It is often desired to use Eq. (40) to compute the finite window jitter variance $\sigma_\delta^2(T)$ for many different values of T. In this case, the matrix exponential e^{AT} must be computed for each desired value of T, but fortunately the P_∞ term (computed via the Lyapunov equation) and A^{-2} terms (which do not depend on T) only require a single computation. However, a further simplification occurs if the T_k lie on a uniformly spaced time grid $T_k = kT_0$, because the matrix exponential e^{AT_0} needs to be computed only once, and then the remaining matrix exponentials can be calculated as $e^{AT_k} = (e^{AT_0})^k$. □

IV. Applications

The state-space formulas developed in Theorem 3.1 and Corollary 3.1 are applied to computing the jitter for a first-order Gauss–Markov process and then to a second-order process for comparison.

A. First-Order Pointing Process

A simple first-order Gauss–Markov process can be used to approximate the behavior of many physical processes and phenomena.[20] Its state-space model is given as

$$\dot{x} = -ax + w \tag{47}$$

$$y = x \tag{48}$$

$$E[w(t)w(t+\tau)] = q \cdot \delta(\tau) \tag{49}$$

The power spectrum is computed as

$$S_n(\omega) = q \cdot |F(j\omega)|^2 \tag{50}$$

where the coloring filter is defined as

$$F(j\omega) = 1/(j\omega + a) \tag{51}$$

Applying method 1 of Theorem 3.1 with the choices $A = -a$, $C = 1$, and $Q = q$ gives the following results:

$$\sigma_n^2 \triangleq = \frac{q}{2a} \tag{52}$$

$$\sigma_m^2(T) = \frac{2(e^{-aT} - 1 + aT)}{a^2T^2} \cdot \sigma_n^2 \tag{53}$$

$$\sigma_\delta^2(T) = \left[1 - \frac{2(e^{-aT} - 1 + aT)}{a^2T^2}\right] \cdot \sigma_n^2 \tag{54}$$

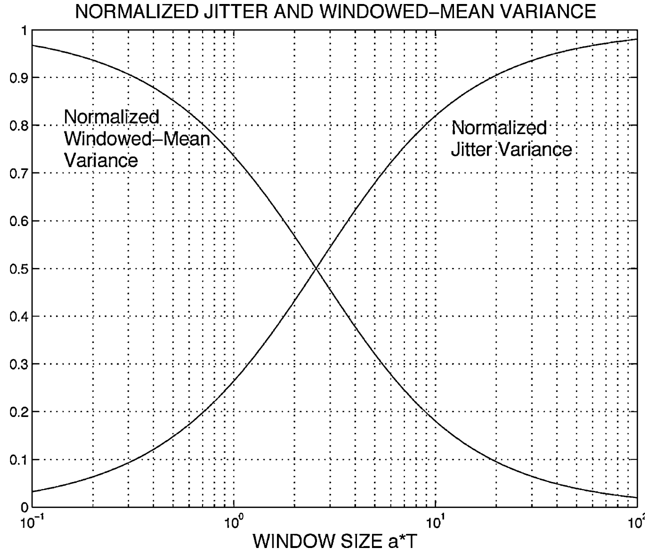

Fig. 4 First-order example: normalized jitter variance $\sigma_\delta^2(T)/\sigma_n^2$ and normalized windowed-mean variance $\sigma_m^2(T)/\sigma_n^2$ vs aT.

Remark 4.1: At this point it is worth noting that Eq. (54) for the scalar problem has *exactly the same structure* as Eq. (40) for the most general state-space problem. In this sense, the main result of this paper can be thought of as an extension of the scalar result to the general matrix case. This is important because an arbitrary rational power spectrum can be obtained for the pointing process $y(t)$ by suitable choice of matrices A, C, and Q in the state-space model (27)–(28). □

The results for Eqs. (53) and (54) are plotted vs aT in Fig. 4 in normalized form for visualization. Defining a time constant for the process as $\tau_c = 1/a$, it is seen that the jitter variance exactly equals the windowed mean variance when the window duration is $T = 2.5569\tau_c$. The jitter variance drops to approximately 10% of the steady-state variance at $T = 0.33\tau_c$ and increases to approximately 90% of the steady-state variance at $T = 19\tau_c$.

B. Second-Order Pointing Process

A second-order pointing process of the following form is studied:

$$\begin{bmatrix} \dot{x}_1 \\ \dot{x}_2 \end{bmatrix} = \begin{bmatrix} 0 & 1 \\ -a^2 & -2a \end{bmatrix} \begin{bmatrix} x_1 \\ x_2 \end{bmatrix} + \begin{bmatrix} 0 \\ w \end{bmatrix} \tag{55}$$

$$y = x_1 \tag{56}$$

$$E[w(t)w(t+\tau)] = q \cdot \delta(\tau) \tag{57}$$

For simplicity, a double real pole at $s = -a$ has been enforced. The power spectrum is computed as

$$S_n(\omega) = q \cdot |H(j\omega)|^2 \tag{58}$$

where the noise coloring filter is defined as

$$H(s) = 1/(s^2 + 2as + a^2) \tag{59}$$

(given as a function of the Laplace variable s). Applying method 1 of Theorem 3.1, with the choices

$$A = \begin{bmatrix} 0 & 1 \\ -a^2 & -2a \end{bmatrix} \tag{60}$$

$$C = [1 \quad 0] \tag{61}$$

$$Q = \begin{bmatrix} 0 & 0 \\ 0 & q \end{bmatrix} \tag{62}$$

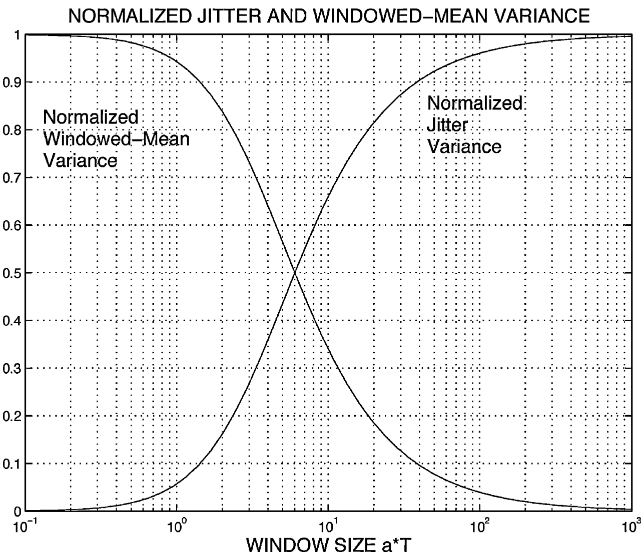

Fig. 5 Second-order example: normalized jitter variance $\sigma_\delta^2(T)/\sigma_n^2$ and windowed-mean variance $\sigma_m^2(T)/\sigma_n^2$ vs aT.

gives the following results:

$$\sigma_n^2 \triangleq = \frac{q}{4a^3} \tag{63}$$

$$\sigma_m^2(T) = \frac{2(3e^{-aT} + aTe^{-aT} - 3 + 2aT)}{a^2T^2} \cdot \sigma_n^2 \tag{64}$$

$$\sigma_\delta^2(T) = \left[1 - \frac{2(3e^{-aT} + aTe^{-aT} - 3 + 2aT)}{a^2T^2}\right] \cdot \sigma_n^2 \tag{65}$$

The results in Eqs. (64) and (65) are plotted vs aT in Fig. 5 in normalized form for visualization. Defining a time constant for the process as $\tau_c = 1/a$, it is seen that the jitter variance equals the windowed mean variance when the window duration is $T = 6.0\tau_c$. The jitter variance drops to approximately 10% of the steady-state variance at $T = 1.43\tau_c$, and increases to approximately 90% of the steady-state variance at $T = 38.7\tau_c$. Compared to the first-order example, the transition is slightly sharper and is shifted toward a longer window duration.

C. Numerical Computation

As a brief numerical comparison, the values $a = 5$, $q = 2$, and $T = 0.286$ are chosen in the present example. Evaluating the close-form symbolic expressions (52)–(54) (obtained using method 1) gives

$$\sigma_n^2 = 4.000000000000000e{-}003 \tag{66}$$

$$\sigma_m^2(T) = 3.599739940495214e{-}003 \tag{67}$$

$$\sigma_\delta^2(T) = 4.002600595047839e{-}004 \tag{68}$$

Evaluating these same quantities using method 3 (forming an augmented matrix exponential, and solving a Lyapunov equation) gives

$$\sigma_n^2 = 3.999999999999998e{-}003 \tag{69}$$

$$\sigma_m^2(T) = 3.599739940495209e{-}003 \tag{70}$$

$$\sigma_\delta^2(T) = 4.002600595047882e{-}004 \tag{71}$$

Finally, evaluating the associated frequency-domain integrals directly by numerical integration (based on MATLAB'S quad.m function, which uses Simpson's rule, set to high-accuracy tolerance = $1e{-}12$) gives

$$\sigma_n^2 = 4.000000000011795e{-}003 \tag{72}$$

$$\sigma_m^2(T) = 3.599739939294205e{-}003 \tag{73}$$

$$\sigma_\delta^2(T) = 4.002600596093323e{-}004 \tag{74}$$

It is seen that all methods agree very well, to at least eight decimals of accuracy. The main limiting factor is the numerical integration, which adheres to a finite tolerance of $1e{-}12$. The two new analytic methods agree to within machine precision (using double-precision arithmetic, that is, epsilon = $2.2e{-}016$).

V. Conclusions

A finite window pointing jitter criterion has been reviewed as an important statistic of a stationary random pointing process that characterizes pointing performance as it affects smearing in imaging instruments with fixed exposure times. As such it has been adopted by several recent JPL/NASA missions for specifying basic mission pointing requirements. The main result of this paper is Theorem 3.1, which gives state-space expressions for evaluating the associated frequency-domain pointing jitter integrals. A particularly concise expression is summarized in Corollary 3.1. The main usefulness is that these expressions are in analytic form and do not require numerical integration.

The present results are in keeping with modern trends to replace frequency-domain integrals with state-space expressions involving only matrix calculations. The new expressions also admit asymptotic short-term and long-term jitter expressions (useful for scaling jitter requirements with time) and have been shown to lead to closed-form symbolic expressions on certain simple examples of general interest.

Appendix: Proof of Theorem 3.1

The arguments used to prove Theorem 3.1 draw upon standard results from optimal estimation and state-space theory. The reader is referred, for example, to Ref. 10, Chaps. 2 and 3, for an overview.

Proof: Assume that at time $t = \tau$ the process state x has already reached steady state, so that its covariance is calculated by solving the Lyapunov equation

$$AP_\infty + P_\infty A^T + Q = 0 \tag{A1}$$

where

$$P_\infty = \lim_{t\to\infty} E[x(t)x(t)^T] \tag{A2}$$

Note that a solution for P_∞ always exists because the matrix A is asymptotically stable.[20] Formula (33) for σ_n^2 (i.e., the steady-state covariance of y) follows directly from Eqs. (A1) and (A2) and output equation (28).

Assume that process y is augmented by a single integrator at its output, to give

$$\dot{\tilde{x}} = \tilde{A}\tilde{x} + \tilde{w} \tag{A3}$$

$$\tilde{x} = \begin{bmatrix} x \\ z \end{bmatrix}, \qquad \tilde{A} = \begin{bmatrix} A & 0 \\ C & 0 \end{bmatrix} \tag{A4}$$

$$\tilde{w} = \begin{bmatrix} w \\ 0 \end{bmatrix}, \qquad \tilde{Q} \triangleq Cov[\tilde{w}] = \begin{bmatrix} Q & 0 \\ 0 & 0 \end{bmatrix} \tag{A5}$$

It will be assumed that the integrator is initialized to zero at time $t = \tau$ so that the state $z(\tau + T)$ is the time integral of y from $t = \tau$ to $t = \tau + T$; that is,

$$z(\tau + T) = \int_\tau^{\tau+T} y(r)\, dr \tag{A6}$$

It is emphasized that because the model (27)–(28) has reached steady state by assumption, the signal $y(t)$ being integrated is a realization of a stationary random process.

This construction of z simplifies the calculation of the statistic $\sigma_m^2(\tau, T)$ through the relations

$$m(\tau, T) = z(\tau + T)/T \tag{A7}$$

$$\sigma_m^2(\tau, T) \triangleq E[m(\tau, T)^2] = P_{zz}(\tau + T)\big/T^2 \tag{A8}$$

where

$$P_{zz}(\tau + T) \triangleq E[z(\tau + T)^2] \tag{A9}$$

that is, it is only left to characterize the covariance P_{zz} of the state z. To this end, the variance of augmented system (A3) propagates from time $t = \tau$ to time $t = \tau + T$ according to the following Lyapunov equation:

$$\dot{\tilde{P}}(t) = \tilde{A}\tilde{P}(t) + \tilde{P}(t)\tilde{A}^T + \tilde{Q} \tag{A10}$$

where

$$\tilde{P}(t) \triangleq E[\tilde{x}(t)\tilde{x}(t)^T] = \begin{bmatrix} P_{xx}(t) & P_{xz}(t) \\ P_{xz}(t)^T & P_{zz}(t) \end{bmatrix} \tag{A11}$$

$$\tilde{P}(\tau) = \begin{bmatrix} P_\infty & 0 \\ 0 & 0 \end{bmatrix} \tag{A12}$$

The initial condition $\tilde{P}(\tau)$ arises from the fact that subsystem (27)–(28) is already in steady state at time $t = \tau$ with covariance P_∞ and from the assumption that the integrator is initialized as $z(\tau) = 0$ with probability one, so that $P_{zz}(\tau) = 0$ and $P_{xz}(\tau) = 0$.

Differential equation (A10) can be written equivalently in terms of the partitioned quantities as follows:

$$\dot{P}_{xx}(t) = AP_{xx}(t) + P_{xx}(t)A^T + Q \tag{A13}$$

$$\dot{P}_{xz}(t) = AP_{xz}(t) + P_{xx}(t)C^T \tag{A14}$$

$$\dot{P}_{zz}(t) = 2CP_{xz}(t) \tag{A15}$$

Using Eq. (A1), one can trivially solve Eq. (A13) with initial condition $P_{xx}(\tau) = P_\infty$ to give

$$P_{xx}(t) = P_\infty \qquad \text{for all} \qquad t \in [\tau, \tau + T] \tag{A16}$$

that is, the original system (27)–(28), which starts in steady state, remains in steady state throughout the entire interval. Substituting Eq. (A16) into Eq. (A14) gives

$$\dot{P}_{xz} = AP_{xz} + P_\infty C^T \tag{A17}$$

Equation (A17) is a system of linear differential equations with constant input and having a zero initial condition $P_{xz}(\tau) = 0$. As such, its solution at any time t can be expressed in terms of the matrix exponential

$$P_{xz}(t) = \left[\int_\tau^t e^{A(t-\ell)}\,\mathrm{d}\ell\right] P_\infty C^T = \left[\int_0^{t-\tau} e^{Ar}\,\mathrm{d}r\right] P_\infty C^T \tag{A18}$$

where use has been made of the change of variable $r = t - \ell$ to simplify the integral. Substituting Eq. (A18) into Eq. (A15) and integrating with respect to time gives

$$P_{zz}(\tau + T) = 2C\left[\int_\tau^{\tau+T}\int_0^{t'-\tau} e^{Ar}\,\mathrm{d}r\,\mathrm{d}t'\right] P_\infty C^T$$
$$= 2C\left[\int_0^T \int_0^s e^{Ar}\,\mathrm{d}r\,\mathrm{d}s\right] P_\infty C^T \tag{A19}$$

where use has been made of the change of variable $s = t' - \tau$ to simplify the integral. Substituting Eq. (A19) into Eq. (A8) gives

$$\sigma_m^2(T) = \frac{2}{T^2}C\left[\int_0^T \int_0^s e^{Ar}\,\mathrm{d}r\,\mathrm{d}s\right] P_\infty C^T \tag{A20}$$

which proves the desired expressions (31)–(34).

Expression (32) is simply a rearrangement of the conservation of variance formula (25).

Method 3 for calculating $\mathcal{H}_T$ from Eqs. (38) and (39) follows as a special case of Theorem 1 in Ref. 21.

Method 1 is proved as follows. By expanding e^{XT} in Eq. (38) into a power series, one can extract the series for $\mathcal{H}_T$ as the upper right $n \times n$ submatrix to give

$$\mathcal{H}_T = (T^2/2!)I + (T^3/3!)A + (T^4/4!)A^2 + \cdots \tag{A21}$$

Multiplying both sides of Eq. (A21) on the left by A^2 and adding $I + AT$ to both sides gives

$$A^2\mathcal{H}_T + I + AT = I + AT + (T^2/2!)A^2 + (T^3/3!)A^3$$
$$+ (T^4/4!)A^4 + \cdots = e^{AT} \tag{A22}$$

where this infinite series has been recognized as a power-series representation of e^{AT}. Solving for $\mathcal{H}_T$ in Eq. (A22) gives

$$\mathcal{H}_T = A^{-2}(e^{AT} - I - AT) \tag{A23}$$

which is Method 1, Eq. (36), as desired. Note that A is always invertible because it is an asymptotically stable matrix which by necessity has no zero eigenvalues.

Consider the well-known Laplace transform expression for the matrix exponential, that is,

$$\mathcal{L}\{e^{AT}\} = (sI - AT)^{-1} \tag{A24}$$

Method 2, Eq. (37), follows by multiplying the Laplace transform in Eq. (A24) by $1/s^2$ to correspond to a double integration in time; that is,

$$\mathcal{L}\left\{\int_0^T \int_0^s e^{Ar}\,\mathrm{d}r\,\mathrm{d}s\right\} = \frac{1}{s^2}(sI - AT)^{-1} \tag{A25}$$

□

Acknowledgments

This research was performed at the Jet Propulsion Laboratory, California Institute of Technology, under contract with the National Aeronautics and Space Administration. The author thanks Sam Sirlin of the Jet Propulsion Laboratory for several technical discussions.

References

[1]Rapier, J. L., "Clutter Leakage Aproximations for Staring Mosaic Sensors with Simultaneous LOS Drift and Jitter," Society of Photo-Optical Instrumenation Engineers, Paper 253-32, San Diego, CA, July 1980.

[2]Hablani, H. B., "Evaluation of Image Stability of a Precision Pointing Spacecraft," *Journal of Guidance, Control, and Dynamics*, Vol. 11, No. 3, 1988, pp. 283–286.

[3]Sirlin, S., and San Martin, A. M., "A New Definition of Pointing Stability," JPL Engineering Memorandum, Jet Propulsion Laboratory, EM 343-1189, Pasadena, CA, March 1990.

[4]Lucke, R. L., Sirlin, S. W., and San Martin, S. M., "New Definitions of Pointing Stability: AC and DC Effects," *Journal of Astronautical Sciences*, Vol. 40, No. 4, 1992, pp. 557–576.

[5]Hyde, P., Perrine, R., and Steuerman, K., "The Observatory Monitoring System: Analysis of Spacecraft Jitter," *Astronomical Data Analysis Software and Systems VI*, edited by G. Hunt and H. E. Payne, ASP Conference Series, Astronomical Society of the Pacific, San Francisco, Vol. 125, 1997.

[6]Bayard, D. S., "Spacecraft Pointing Control Criteria for High Resolution Spectroscopy," *IEEE Transactions on Aerospace and Electronic Systems*, Vol. 35, No. 2, 1999, pp. 637–644.

[7]Bayard, D. S., "A State-Space Approach to Computing Spacecraft Pointing Jitter," AIAA Paper 2003-5782, Aug. 2003.

[8]Pittelkau, M. E., “Pointing Error Definitions, Metrics, and Algorithms,” American Astronomical Society, AAS 03-559, Aug. 2003.

[9]Lee, A. Y., Yu, J. W., Kahn, P. B., and Stoller, R. L., “Preliminary Spacecraft Pointing Requirements Error Budget for the Space Interferometry Mission,” *1999 IEEE Conference Aerospace Systems*, Inst. of Electrical and Electronics Engineers, Piscataway, NJ, 1999.

[10]Lewis, F. L., *Optimal Estimation, with an Introduction to Stochastic Control Theory*, Wiley, New York, 1986, Chaps. 2, 3.

[11]Bayard, D. S., “A Simple Analytic Method for Computing Instrument Pointing Jitter,” Jet Propulsion Laboratory, Internal Document D-19967, Pasadena, CA, Nov. 2000.

[12]Papoulis, A., Probability, Random Variables, and Stochastic Processes, McGraw–Hill, New York, 1965, Chap. 9.

[13]Cassini Project, “Guidance and Analysis Book: Final,” Jet Propulsion Laboratory, Internal Document D-7841, Pasadena, CA, Sept. 1994.

[14]Kia, T., Bayard, D. S., and Tolivar, F., “A Precision Pointing Control System for the Space Infrared Telescope Facility,” American Astronomical Society, AAS 97-067, Feb. 1997.

[15]Bayard, D. S., “An Overview of the Pointing Control System for NASA’s Space Infra-Red Telescope Facility (SIRTF),” AIAA Paper 2003-5832, Aug. 2003.

[16]Baiocco, P., and Sevaston, G., “On the Attitude Control of a High-Precision Space Interferometer,” *Space Guidance, Control, and Tracking*, Vol. 1949, 1993, pp. 92–107.

[17]Carlson, A. E., *Communication Systems*, McGraw–Hill, New York, 1975, Chap. 2.

[18]Moler, C., and Van Loan, C., “Nineteen Dubious Ways to Compute the Exponential of a Matrix,” *SIAM Review*, Vol. 20, No. 4, 1978, pp. 801–836.

[19]Laub, A. J., “A Schur Method for Solving Algebraic Riccati Equations,” *IEEE Transactions on Automatic Control*, Vol. AC-24, No. 6, 1979, pp. 913–921.

[20]Gelb, A. (ed.), *Applied Optimal Estimation,* MIT Press, Cambridge, MS, 1984, Chap. 2.

[21]Van Loan, C. F., “Computing Integrals Involving the Matrix Exponential,” *IEEE Transactions on Automatic Control*, Vol. AC-23, No. 3, 1978, pp. 395–404.